International Journal for Innovative Engineering and Management Research
PEER REVIEWED OPEN ACCESS INTERNATIONAL JOURNAL
www.ijiemr.org

COPY RIGHT

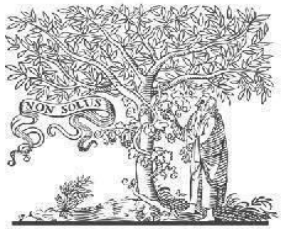

ELSEVIER SSRN

IJIEMR Transactions, online available on 30th Dec 2022. Link

https://ijiemr.org/downloads.php?vol=Volume-11&issue= Issue12

DOI:10.48047/IJIEMR/V11/ISSUE12/384

Title: "OPTIMIZATION OF A SINGLE-ORIFICE PLATE UNDER CAVITATION CONDITIONS USING THE NEIGHBORHOOD CULTIVATION GENETIC ALGORITHM"

Volume 11, ISSUE 12, Pages: 3256- 3262

Paper Authors
C. Syamsundar

USE THIS BARCODE TO ACCESS YOUR ONLINE PAPER

To Secure Your Paper as Per UGC Guidelines We Are Providing A ElectronicBar code

International Journal for Innovative Engineering and Management Research
PEER REVIEWED OPEN ACCESS INTERNATIONAL JOURNAL
www.ijiemr.org

OPTIMIZATION OF A SINGLE-ORIFICE PLATE UNDER CAVITATION CONDITIONS USING THE NEIGHBORHOOD CULTIVATION GENETIC ALGORITHM

C. Syamsundar
Department of Mechanical Engineering, CMR Engineering College, Hyderabad, Telangana 501 401, India
syamsundariitm@gmail.com

Abstract

The single-orifice plate is extensively employed in nuclear power plant piping systems for fluid throttling and depressurization, yet the cavitation it induces can lead to significant pipeline vibrations. This study aims to identify optimal single-orifice plate designs with minimized cavitation potential. A novel single-orifice plate featuring a convergent-flat-divergent hole was modeled, and a multi-objective optimization approach was proposed to refine its shape. Computational fluid dynamics (CFD) methods were utilized to capture fluid dynamics, with cavitation indexes such as the reciprocal cavitation number and the developmental integral serving as objectives for the optimization algorithm. Through this process, two non-dominant designs were identified, showcasing considerable reductions in cavitation indexes at a Reynolds number (Re) of $1 * 10^5$ based on fluid velocity.

Additionally, sensitivity analyses and assessments of temperature effects were conducted. Results underscored the significant influence of the convergent angle of the single-orifice plate on cavitation behavior. Optimized designs demonstrated decreased downstream jet areas and reduced upstream pressure. Temperature effects indicated higher liquid water temperatures correlate with increased cavitation susceptibility, whereas this relationship is diametric for constant fluid velocities. Furthermore, regression models were developed to establish mathematical relationships between temperature and cavitation indexes.

Keywords: Single-orifice plate; Cavitation; Shape optimization; Neighborhood cultivation genetic algorithm; Computational fluid dynamics

1. Introduction

The single-orifice plate (SOP) has been extensively encountered in the piping system of nuclear power plants **[Shan et al., 2023; Harris, 2022]**. One of the main functions of SOP is the throttling effect, reducing the coolant flow and the circuit pressure in pipelines **[Ebrahimi et al., 2021]**. With an orifice plate, the fluid pressure in the pipeline may drop sharply due to the sudden contraction of the stream tube and then recover gradually.

The dimensionless number, pressure loss coefficient determined by the fully developed recovery pressure and the upstream pressure of SOPs, can be used to

characterize the capability of pressure reduction **[Ai and Wu, 2024; Li et al., 2019]**. According to the numerical results of CFD, Shaaban **[Shaaban, 2019]** found that the pressure loss coefficient is sensitive to the convergent angle of the orifice plate. When the convergent and divergent angles are 50^0 and 7^0 at Re = 3.5 X 10^{-4}, respectively, the minimum value of the pressure loss coefficient can be obtained. Several numerical simulations using the realizable $k-\varepsilon$ viscosity model were carried out by Araoye et al. to investigate the influences of various parameters such as the pipe flow velocity, orifice spacing, and orifice plate diameter on the pressure distributions **[Araoye et al., 2017]**. The numerical results indicate no substantial effect of the orifice internal on the total pressure drop.

As a common and inevitable hydrodynamic phenomenon, cavitation occurs in nearly all hydraulic machinery, such as hydrofoils, centrifugal pumps, and turbines **[Liu et al., 2019; Sun and Tan, 2020],** and pipes with SOP. Cavitation is a process that includes vaporization, bubble formation, and collapse when the partial pressure is reduced below the saturation pressure. With the advent of cavitation, some potential problems composing noise, pressure undulation, structure vibration, and even erosion on the structure surface may be triggered **[Liu et al., 2019]**. Accordingly, controlling the cavitation degree and getting insight into the cavitation mechanism is indispensable. Regarding the low-pressure regions as one of the indexes of cavitation intensity, Cappa et al. **[Cappa, 2020]** found that the greater the thickness of SOP, the more volume of cavities produced. **Li et al. [2017]** studied the cavitation structures and optimized the geometrical parameters of SOP by surrogate model and global sensitivity assessment. The results indicate that the throat and inlet diameters significantly influence the cavity size. In contrast, the throat length has little effect on both flow rate and cavitation intensity.

A multi-objective morphological optimization of SOP based on the neighbourhood cultivation genetic algorithm (NCGA). Two optimal designs of SOPs were obtained in this study.

2. Mathematical model

2.1 Flow governing equations

Neglecting thermal convection, heat conduction, and compressibility, the physical quantities in the pipeline below can be acquired by solving the incompressible Reynolds averaged Navier-Stokes equation.

2.2 Cavitation intensity and loss coefficient

The potential of cavitation inside the pipe devices is characterized by a dimensionless number, identified as cavitation number (C_v), which can be expressed as:

$$C_v = \frac{p - p_v}{\frac{1}{2}\rho V^2} \tag{12}$$

Where p is the centerline absolute pressure, p_v is the saturated vapor pressure of the fluid at operating temperature, and V is the flow speed. With the decreasing value of C_v, the probability of cavitation increases monotonously. The minimum value of the cavitation number, C_{vmin}, is an influential evaluation index. According to Equation (12), C_v varies with the downstream section position. Naturally, a dimensionless integral value Ic, which reflects the summation of local cavitation degree, is defined, named cavitation intensity, and normalized by the pipe inner diameter:

$$I_c = \int_0^{L_u} C_v^{-1}(x)\frac{x}{D}dx \tag{13}$$

Where the integral upper L_u corresponds to the downstream pressure recovery location, it can be inferred that the value of I_c is positively related to the overall cavitation degree. As the liquid passes through the SOP, the hydraulic pressure drops sharply and gradually returns to the outlet pressure. The loss of coefficient K depicts this pressure change:

$$K = \frac{p_u - p_d}{\frac{1}{2}\rho V_m^2} \tag{14}$$

Where p_u, p_d are the centerline absolute pressure at two sections, respectively, V_m is the mean velocity.

3. Parameter and optimization algorithm

There are three steps: numerical calculation, data process, and optimization. In the first step, based on the parametric geometry model, the automatic meshing is carried out, and the finite volume solver is used to obtain the physical quantities such as the pressure and the velocity. In the second step, the cavitation indexes are extracted. In the last step, the multi-objective optimization is implemented based on the Neighborhood Cultivation Genetic Algorithm to receive the non-dominant solutions.

The example of SOP's general profile and three-dimensional geometry is shown in Figure 1. The present study proposes a universal geometry with a convergent-flat-divergent hole. The inner diameter of the pipeline is D_p, the total thickness of SOP is t_s, the diameter of the hole is D_f, the thickness of the flat edge is t_f, the angle between convergent and divergent and flat edges are a and b, respectively.

The present study treats Dp, Df, and ts as constants according to engineering constraints. Neighborhood Cultivation Genetic Algorithm (NCGA) is adopted for

global optimization, a multi-objective exploratory methodology **[Watanabe et al., 2022]**. The calculation process of NCGA is stated as follows:

Steps

1. **Initialization:** Create an original population P_0 with N size, set generation g=0. Calculate the fitness values of individuals in P_0. Assign P_0 to A_0 (archive).
2. $\boldsymbol{g = g+1,\ P_g = A_{g-1}}$
3. **Sorting:** Rank the individuals of P_g according to the value of the chosen objective. The desired objective varies with the generation. If there are two objectives, the chosen objective in the first generation is the first objects, and the second is chosen when $g = 2$. In turn, the first objective is chosen again when $g = 3$.
4. **Dividing:** Separate P_g into two groups, which are selected from the sorted individuals.
5. **Crossover and mutation (Genetic algorithm):** The crossover and mutation operations are executed for each group. Produce two child groups and abandon the parent groups.
6. **Assembly:** Gather the child groups generated in Step 5 to form a new P_g.
7. **Selection operation:** Assemble P_g and A_{g-1} to form 2 N individuals. The environment selection is carried out to reduce the number of individuals to N. Ultimately, A_g is generated.
8. **Termination:** Determine whether the convergence criterion (number of generation or relative errors) is reached. If the criterion is satisfied, the process can be finished. Otherwise, the simulation goes to Step 2.

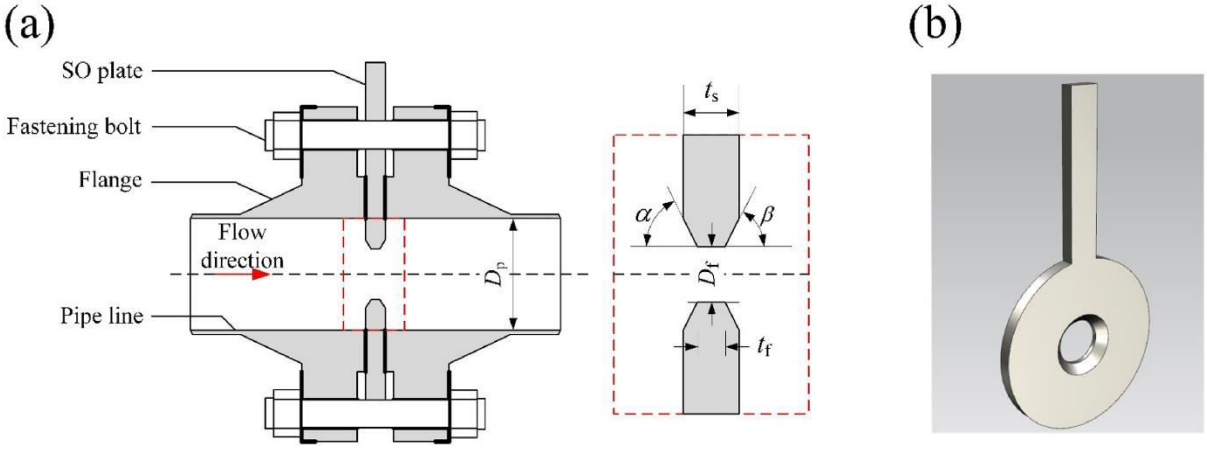

Figure 1. (a) Diagram of SOP, (b) three-dimensional geometry.

4. Validation

A calculation of the CFD was presented to obtain the cavitation state of a pipeline with SOP. CFD is an appropriate method for this complicated flow distribution, and a

validated commercial CFD analysis program was used in this calculation. All calculations were carried out at temperature T_s =300K. At the standard atmospheric pressure (approximately 101.325kPa) condition, the density of the incompressible water is 998 kg/m^3, the viscosity is 0.001 Pa s, and the saturated vapor pressure is 3.54kPa. ANSYS ICEM CFD was used to discrete the fluid domain, and the high-quality entire quadrilateral structured grid was obtained. Before CFD was calculated, a mesh independence analysis and a model validation were conducted, respectively.

The boundaries specified in numerical modeling are illustrated in Figure 2. The inlet is subject to velocity inlet boundary conditions. In contrast, the no-slip and insulation conditions are endowed at pipe and SOP walls. The outlet is assumed to be a pressure outlet condition with zero pressure. The middle meshing strategy was chosen because it required less calculation ¼ time and power.

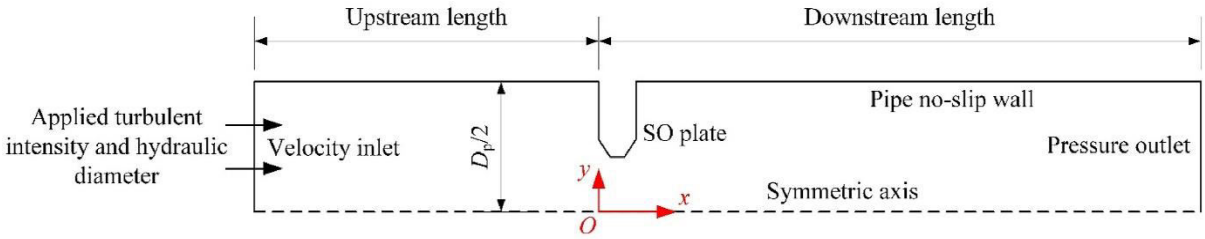

Figure 2. Computational domain.

5. Results and discussion

In the present work, D_p is 180.3 mm, and t_s is 10.0 mm. The upstream and downstream lengths of the pipeline are $10D_p$ and $20D_p$, respectively. Re is 1 x 10^5, and the corresponding inlet velocity and turbulence intensity are 0.5546 m/s and 3.8%, respectively.

The velocity contours of the original and optimized SOPs at Re =1x10^5 were illustrated in Figure 3(a). The jet flow can be observed induced by the SOPs. The jets of the optimized SOPs consist of smaller high-speed areas compared to the plane of the original SOP, indicating a smaller pressure range and a lower possibility of Cavitation of the optimized SOPs. Meanwhile, the subordinate speed wakes farther downstream of SOPs, which are restricted in the optimized designs.

Figure 3(b) shows the static pressure distribution for the original and the optimized SOPs at the same Reynolds number. The static pressure upstream of the original SOP is more intense than the one in Cases 1 and 2, which indicates that the convergence angle effectively alleviates the high-pressure area. In the meantime, the low-pressure regions downstream optimized SOPs are reduced significantly due to the altering of hole geometry. Furthermore, a greater divergent angle of Case 2 reduces the low-pressure area near the downstream boundary of SOP. Additionally, no apparent change in the static pressure distribution downstream of SOP was observed.

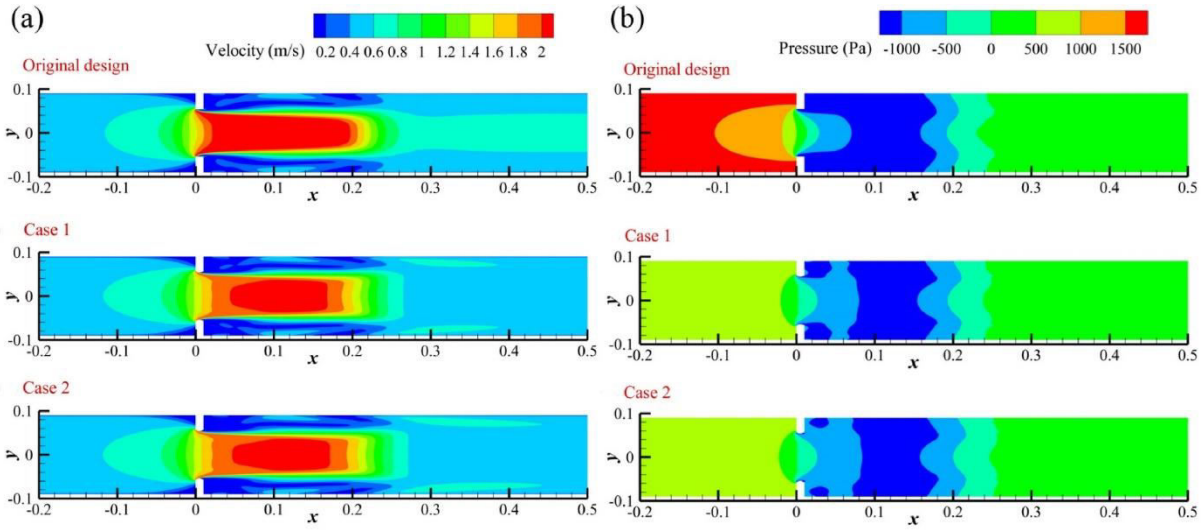

Figure 3. Velocity and pressure contours of the origin and non-dominant designs.

6. Conclusion

The single-orifice plate is widely applied in pipeline systems of nuclear power plants. This research aims to obtain the single- orifice plate with the lowest cavitation potential and explore the influences of geometric parameters and temperature on cavitation behaviour. The reciprocal cavitation number C_r and its integral I_c are regarded as cavitation indexes, and the cavitation performance of a single-orifice plate was evaluated utilizing a multi-objective optimization method (NCGA). The conclusions of this paper can be summarized as follows:

1. Two non-dominant designs, Case 1 and 2, were extracted from the Pareto solutions. For Case 1, the attainable reduction in C and I_c is 23.2% and 63.1%, respectively. For Case 2, the decrease in C_r and I_c is 24.1% and 62.1%, respectively.

2. Global sensitivity analysis showed that the convergent angle of the SOP is the most crucial parameter on the cavitation indexes. At the same time, the flat edge length and the divergent angle of the SOP have marginal influences on the cavitation performance.

3. The jet areas of the two optimal morphologies of single-orifice plates are smaller than the one of the original ones, and the upstream pressure was reduced significantly.

7. References

1. F. Shan, A. Fujishiro, T. Tsuneyoshi, Y. Tsuji, Particle image velocimetry measurements of flow field behind a circular square-edged orifice in a round pipe, Exp. Fluid 54 (2023) 1553.

2. M.R. Harris, Orifice design, in: Orifice Plates and Venture Tube. Experimental Fluid Mechanics, Springer, Cham, 2015. 1843Y. Zhang, J. Lai, C. He et al. Nuclear Engineering and Technology 54 (2022) 1835e1844

3. B. Ebrahimi, G. He, Y. Tang, M. Franchek, D. Liu, j. Pickett, F. Springett, D.

Franklin, Characterization of high-pressure cavitating flow through a thick orifice plate in a pipe of constant cross-section, Int. J. Therm. Sci. 114 (2021) 229e240.

4. W.Z. Ai, J.H. Wu, Comparison of hydraulic characteristics between orifice plate and plug, J. Shanghai Jiaot. Univ. 19 (4) (2024) 476e480.

5. M. Li, A. Bussonniere, M. Bronson, Z. Xu, Q. Liu, Study of venture tube geometry on the hydrodynamic cavitation to generate microbubbles, Miner. Eng. 132 (2019) 268e274.

6. S. Shaaban, On the performance of perforated plate with optimized hole geometry, Flow Meas. Instrum. 46 (2019) 44e50.

7. A.A. Araoye, H.M. Badr, W.H. Ahmed, Investigation of flow through multi-stage restricting orifices, Ann. Nucl. Energy 104 (2017) 75e90.

8. M. Liu, L. Tan, S. Cao, Dynamic mode decomposition of cavitating flow around ALE 15 hydrofoil, Renew—Energy 139 (2019) 214e227.

9. W. Sun, L. Tan, Cavitation-vortex-pressure fluctuation interaction in a centrifugal pump using bubble rotation modified cavitation model under partial load, J. Fluid Eng. 142 (2020), 051206.

10. M. Liu, L. Tan, S. Cao, Cavitation-vortex-turbulence interaction and one-dimensional model prediction of pressure for hydrofoil ALE 15 by large eddy simulation, J. Fluid Eng. 141 (2019), 021103.

11. O.A.P. Cappa, T.V.R. Soeira, A.L.A. Simoes, G.B.L. Junior, J.C.S.I. Goncalves, Experimental and computational analyses for induced cavitating flows in orifice plates, Braz. J. Chem. Eng. 37 (2020) 89e99.

12. X. Li, B. Huang, T. Chen, Y. Liu, S. Qiu, J. Zhao, Combined experimental and computational investigation of the cavitating flow in an orifice plate with particular emphasis on surrogate-based optimization method, J. Mech. Sci. Technol. 31 (1) (2017) 269e279.

13. S. Watanabe, T. Hiroyasu, M. Miki, Neighborhood cultivation genetic algorithm for multi-objective optimization problems, in Proceedings of the 4th Asia-Pacific Conference on Simulated Evolution and Learning, SEAL-2002, 2022, pp. 198e202.